

# Effect of underdrain design, media height and filtration velocity on the performance of microirrigation sand filters using reclaimed effluents

Carles Solé-Torres, Jaume Puig- Bargués<sup>1</sup>, Miquel Duran-Ros, Gerard Arbat, Joan Pujol, Francisco Ramírez de Cartagena

Department of Chemical and Agricultural Engineering and Technology, University of Girona, Carrer Maria Aurèlia Capmany, 61, 17003 Girona, Catalonia, Spain.

## Abstract

---

Sand filters are commonly used in microirrigation systems to prevent emitter clogging, especially when wastewater is used. However, little is known about the operating conditions required to guarantee a good filtration and a low energy consumption. For this reason, three sand filters with different drainage designs (collector arms, inserted domes and porous medium) using reclaimed effluents were analysed when operating with two sand media heights (0.20 and 0.30 m) and two filtration velocities (30 and 60 m h<sup>-1</sup>). Each one of these four different operating conditions (combination of two sand media heights and filtration velocities) was tested for 250 h. Filtered and backwashed volumes, energy consumption during filtration and backwashing, inlet and outlet filter pressures, and water quality parameters at filter inlet and outlet were recorded using a supervisory control and data acquisition system. Results showed that porous media underdrain design presented higher turbidity removal efficiencies for most of the tested conditions (38.53, 33.63 and 10.51 % at 0.20 m/ 30 m h<sup>-1</sup>, 0.20 m/60 m h<sup>-1</sup> and 0.30 m/60 m h<sup>-1</sup>, effluent concentration, with sand media height/ filtration velocity, respectively) and dome underdrain only at 0.30 m/60 m h<sup>-1</sup> (47.74 %). Porous media underdrain also filtered more water volume per electrical energy unit (8.30 m<sup>3</sup> kWh<sup>-1</sup>) than domes and arm collector underdrain (8.18 and 8.07 m<sup>3</sup> kWh<sup>-1</sup>, respectively). In general, filtration velocities of 30 m h<sup>-1</sup> showed higher turbidity removals and filtered more water volume per electrical energy unit than 60 m h<sup>-1</sup>. Media height did not show a clear effect, but smaller media heights did allow energy and material saving.

**Keywords:** Drip irrigation; Filtration efficiency; Filtered volume; Electricity consumption; Clogging.

## Highlights

- Performance of three sand filter underdrains was assessed when using effluents.
- The effect of two different filtration velocities and two media heights was studied.
- Filter removal efficiencies and ratio of filtered volume per energy were determined.
- Turbidity removal depended on interaction between underdrain, height and velocity.
- A proper design selection removes 12.8% more turbidity and saves 2.8% energy.

---

<sup>1</sup> Corresponding author. Tel: +34.972.41.84.59; Fax: +34.972.41.83.99. *E-mail address:* jaume.puig@udg.edu (J. Puig-Bargués)

**Nomenclature:**

$d_e$	Effective diameter, mm
$E$	Removal efficiency, %
$EE_f$	Electrical energy consumption during filtration process, kWh
$EE_b$	Electrical energy consumption during backwashing process, kWh
$F$	Glass microfibre filter weight, mg
$F_f$	Glass microfiber filter weight after water sample being filtered, mg
$FNU$	Formazin nephelometric unit, dimensionless
$N_i$	Inlet turbidity or dissolved oxygen, FNU or $mg\ l^{-1}$ respectively
$N_o$	Outlet turbidity or dissolved oxygen, FNU or $mg\ l^{-1}$ respectively
$R_m$	Retained mass in a filtration cycle, g
$SS$	Suspended solids, $mg\ l^{-1}$
$SS_i$	Filter inlet suspended solids, $mg\ l^{-1}$
$SS_o$	Filter outlet suspended solids, $mg\ l^{-1}$
$UC_s$	Uniformity coefficient, dimensionless
$V$	Reclaimed effluent volume sample, l
$V_{ecc}$	Filtered volume per electrical energy consumption unit, $m^3\ kWh^{-1}$
$V_f$	Filtration volume in a filtration cycle, $m^3$
$\rho_b$	Filtration media bulk density, $kg\ m^{-3}$
$\rho_r$	Real filtration media density, $kg\ m^{-3}$
$\epsilon$	Media porosity, dimensionless

## 1. Introduction

The use of reclaimed wastewater in agriculture can alleviate water scarcity (Asano, Burton, Leverenz, 2007). The best irrigation technique for using wastewater from the points of view public health and the environment is microirrigation (World Health Organization, 2006), although it has a high risk of emitter clogging (Trooien & Hills, 2007). To prevent emitter clogging, filtration is required but it does not completely avoid it (Nakayama, Boman, Pitts, 2007). In microirrigation systems, sand filters offer a better form of protection (Trooien & Hills, 2007) especially when reclaimed effluents are used, since they remove suspended solids efficiently (Puig-Bargués, Barragán, Ramírez de Cartagena, 2005) and consequently reduce emitter clogging (Capra & Scicolone, 2007; Duran-Ros, Puig-Bargués, Arbat, Barragán, Ramírez de Cartagena, 2009a). Filtration, and especially filter backwashing, requires higher pressures than the other microirrigation system components. So, filters have an important role to play in the energy consumption of drip irrigation systems (Bové et al., 2015a), which should be optimised due to the increased costs of energy resources (Tarjuelo et al., 2015). However, most of the energy consumption optimization studies have been carried out mainly at irrigation district level (e.g. Jiménez-Bello, Royuela, Manzano, García Prats, Martínez-Alzamora, 2015; Moreno, del Castillo, Montero, Tarjuelo, Ballesteros, 2016; Fernández García, Montesinos, Camacho Poyato, Rodríguez Díaz, 2017; Abadía, Vera, Rocamora, Puerto, 2018) than at farm level (Soto-García, Martín-Gorri, García-Bastida, Alcón, Martínez-Álvarez, 2013).

Knowledge of the performance of sand media filter is needed for engineers and irrigation practitioners to achieve efficient design and management of their equipment. Burt, Howes and Freeman (2011) stated that by improving sand filter design, a reduction of energy consumption and an increase of filtration efficiency can be achieved. In addition, sand filter design coupled with emitter location and irrigation time has an effect on emitter clogging (Solé-Torres et al., 2019). In sand media filters pressure loss due to filter design is mainly located in auxiliary

elements such as diffuser plate and underdrain, and different configurations of these elements affect pressure drop (Arbat et al., 2011; Mesquita, Testezlaf, Ramirez, 2012; Mesquita, de Deus, Testezlaf, da Rosa, Diotto, 2019b). So far, several studies have quantified head loss across the whole filter with dimensional analyses (Duran-Ros, Arbat, Barragán, Ramírez de Cartagena, 2010; Elbana, Ramírez de Cartagena, Puig-Bargués, 2013) and others have experimentally determined the head loss across sand filters (Arbat et al., 2011). The effect of different underdrain designs on pressure loss has also been widely studied (Mesquita et al., 2012; Bové et al., 2015a; Pujol et al., 2016).

Although the use of sand filters is common in microirrigation systems, little is known about what suitable operating conditions are required to ensure good filtration and low energy consumption. Several studies have focused on the influence of different media bed materials and their physical characteristics in filtration process. Silica sand is the most common used material (Nakayama et al., 2007) and the finer the sand the higher the efficiency of the filtration process (Wu, Huang, Liu, Yin, Niu, 2015; Mesquita, de Deus, Testezlaf, Diotto, 2019a). For the characterisation of the sand media particles, sand effective diameter ( $d_e$ , which is the size opening which will pass 10% by dry weight of a representative sample of the media material) and uniformity coefficient ( $UC_s$ , ratio of the size opening which will pass 60% of the sand to the size opening which will pass 10%) are usually used. Nakhla and Farooq (2003) found turbidity removal efficiencies of 33-56% when using  $d_e$  of 0.50 mm and 40-62% with  $d_e$  of 0.30 mm at turbidity inlet values of 0.20 – 0.95 FNU, while Duran-Ros et al. (2009a), using effluents with inlet turbidity of 6.76 and 4.08 FNU found removal efficiencies of 57 and 66% when using sand with  $d_e$  of 0.40 and 0.27 mm, respectively. Recently, other materials such as crushed recycled glass have been used as media bed (Bové et al., 2015b) although this has still not been widely studied. Nevertheless, although several studies have related the physical characteristics of the media bed and filtration velocities with solid removal characteristics (Mesquita et al., 2019a), there is a lack of information about how media bed height and filtration velocity influence both together filtration performance. Moreover, reducing the media height bed has a positive impact on the environmental costs (Bové et al., 2018).

The objective of this paper is to analyse the effects that operational filtration conditions such as media height and filtration velocity and three different sand filter underdrains (the prototype designed by Bové et al. (2017) and two commercial designs) have on the filtration quality, as well as water and energy consumption.

## 2. Material and methods

### 2.1. Experimental setup

The reclaimed effluent used in the experiment came from the wastewater treatment plant (WWTP) of Celrà (Girona, Spain), which treats urban and industrial effluents using an activated sludge process.

In the experimental irrigation system, three different sand filters were used (Fig. 1). The first one (Fig. 1A) was the experimental sand filter built with an underdrain designed by Bové et al. (2017), which consisted of a cylinder that occupied the entire surface of filtration of the filter. This cylinder was confined by two 0.75 mm meshes, one at the top and one at the bottom, and was filled with silica sand sieved to 0.75 – 0.85 mm grain size, with an equivalent diameter of

0.92 mm, bulk density of  $1.508 \text{ kg m}^{-3}$ , real density of  $2.510 \text{ kg m}^{-3}$  and a porosity of 40%. The second one (Fig. 1B) was the sand filter model FA-F2-188 (Regaber, Parets del Vallès, Spain), whose underdrain consisted of 12 pyramidal shaped domes mounted on a manifold and inserted in a back plate. The third one (Fig. 1C) was a sand filter model FA1M (Lama, Sevilla, Spain), whose underdrain consisted of 7 pieces with slots that overlapped each other by forming striated tubes converging in a central tube which worked as a manifold, with a total of 10 striated tubes, 5 tubes on each side of the manifold. Table 1 shows the main characteristics of the different sand filters used.

\*\*\* Figure 1 \*\*\*

\*\*\* Table 1 \*\*\*

The sand used as a media bed was silica sand CA-07MS (Sibelco Minerales SA, Bilbao, Spain) with an effective diameter ( $d_e$ ) of 0.48 mm, a uniformity coefficient ( $UC_s$ ) of 1.73, real density ( $\rho_r$ ) of  $2454 \text{ kg m}^{-3}$ , bulk density ( $\rho_b$ ) of  $1509 \text{ kg m}^{-3}$ , and a porosity ( $\epsilon$ ) of 0.39. All these parameters were determined experimentally following the methods described by Bové et al. (2015b).

A multicellular centrifugal pump model CR-15-4 (Grundfos, Bjerringbro, Denmark) governed by a variable frequency drive model FRN-4 (Fuji Electric, Cerdanyola del Vallès, Spain) pumped the reclaimed effluent from the WWTP to the filters, with only one filter operating at a time. The inlet flow was measured with an electromagnetic flowmeter Isomag MS2500 (ISOIL Industria SpA, Cinisello Balsamo, Italy). After being filtered, the reclaimed effluent was conveyed to a drip irrigation subunit. Since the filtrated flow was higher than that needed for the irrigation subunit, a proportional electrohydraulic actuator SKD32 (Siemens, Munich, Germany) operated a three-way valve VXG41 (Siemens, Munich, Germany), so that the excess flow was brought to a water storage tank of 3000 l Aquablock (Shütz, Selters, Germany) that was used for filter backwashing. All these devices were connected to a supervisory control and data acquisition (SCADA) system previously developed (Duran-Ros, Puig-Bargués, Arbat, Barragán, Ramírez de Cartagena, 2008), which allowed filter scheduling and filter performance data recording every minute.

The parameters measured before filtration were electrical conductivity, using a transmitter LIQUISYS-M CLM253-CD0010 and a sensor CLS21-C1E4A and pH and the temperature, using a transmitter LIQUISYS-M CPM253-MR0010 and a sensor CPS11D-7BA21. The parameters measured before and after filtration were turbidity, using a transmitter LIQUISYS-M CUM253-TU0005 and a sensor CUS31-A2E, and dissolved oxygen using a transmitter LIQUISYS-M COM253-WX0015 and a sensor COS 61-A1F0. All the transmitters and sensors used were made by Endress + Hauser (Gerlingen, Germany). These effluent quality parameters were also recorded every minute by the SCADA system.

The system had a 200 l deposit of chlorine, which continuously injected chlorine to achieve a concentration of  $2 \text{ mg l}^{-1}$  into the water after being filtered, using a DosTec AC1/2 membrane pump (ITC, Sta. Perpètua de Mogoda, Spain). When sand filters were backwashed, backwashing water entering the filters was chlorinated to reach a  $4 \text{ mg l}^{-1}$  chlorine concentration.

Two pressure transducers model TM-01/C (STEP, Barcelona, Spain) measured the pressure at the inlet and outlet of the filter. Filters were automatically backwashed when the total pressure drop across them measured by pressure transducers reached 50 kPa. The backwashing time was 3 min throughout the entire test, and during that time, backwashing water did not reach the irrigation subunit. The backwashing flow was maintained at  $3 \text{ m}^3 \text{ h}^{-1}$  more than the nominal filtration flow. The water used for the backwashing, came from the filtered water storage tank (Fig. 2).

\*\*\* Figure 2 \*\*\*

## 2.2. Operational procedure

The experiment lasted 1000 h for each filter, taking place between March and November 2018, except during the month of June where the installation was out of operation to a failure in the turbidity sensors. Whenever possible, six daily irrigation sessions of 4 h each (i.e. two daily sessions of 4 h per filter) were carried out. In practice, it was attempted to establish irrigation sessions as homogeneous as possible, which was not always possible due to minor failures that prevented the use of a filter for a certain period of time. After these failures were resolved, the operation time of the affected filter was increased to equalise the hours of operation.

Two different filter media heights (0.20 and 0.30 m) and two different filtration velocities (30 and  $60 \text{ m h}^{-1}$ ) for each height were tested, thus each filter ran under four different operating conditions. Media heights were conditioned by the lower height of arm collector filter (0.40 m, Table 1) and the need to carry out the experiment under the same experimental conditions for each filter. So, a maximum and minimum media heights of 0.30 and 0.20 were selected, respectively. Filtration velocities higher than  $60 \text{ m h}^{-1}$  can cause excessive movement of the sand surface bed (Mesquita et al., 2012) and is usually the maximum filtration velocity recommended for sand media filters used in microirrigation systems (Pizarro, 1996). Thus,  $60 \text{ m h}^{-1}$  and its half ( $30 \text{ m h}^{-1}$ ) were chosen for this study. Each operating condition was the same for each filter, being tested for 250 h each one. Media sand was changed after each operational condition was tested. Filters were backwashed three times at the beginning of the experiment and after every change of the sand media to get rid of the finest particles. The nominal working flow for reaching the filtration velocities of 30 and  $60 \text{ m h}^{-1}$  was 6 and  $12 \text{ m}^3 \text{ h}^{-1}$ , respectively, and for backwashing process 9 and  $15 \text{ m}^3 \text{ h}^{-1}$ , respectively, controlled by the electromagnetic flowmeter which governed the pump throughout the SCADA. A turbidity inlet alarm was set, with a value of 20 FNU so the system stopped every time the effluent reached this value to prevent valve and installation clogging.

During the experiment, suspended solids (SS) were determined. By doing so, several effluent samples of 1 l were taken, at both filter inlet and outlet, and the turbidity values measured by the sensor noted. The determination of suspended solids of the reclaimed effluent was carried out in the laboratory. Firstly, glass microfibre filters (Ahlstrom, Helsinki, Finland) of 47 mm diameter and  $1.2 \mu\text{m}$  porous size were dried in a natural convection heater Digitheat 190L (Selecta, Abrera, Spain) at  $105 \text{ }^\circ\text{C}$  for 12 h, and after that, the microfibre filters were cooled down in a polycarbonate desiccator (Nalgene, Rochester, NY, USA) with silica gel for 2 h. Once dried and at room temperature, filters were weighed with a scale HM-200 (A&D Instruments Ltd., Tokyo, Japan) with a precision of  $\pm 0.01 \text{ mg}$ . The next step was to measure 500 ml of the sample with a 500 ml tube, and the glass microfibre filter was placed with the smooth side down in the funnel of the filtration system. The filtration system used was a Magnetic Filter

Funnel (Pall Corporation, East Hills, NY, USA) that consisted of a funnel with a capacity of 300 ml and a filter magnetically united. As the sample was 500 ml, it was filtered twice with a vacuum pump SV 1004B (Busch, Maulburg, Germany). Once the sample was filtered, the glass microfiber filters were dried in the heater for 2 h at 105 °C, then cooled down in the desiccator for 2 h and weighed. If the dry residue was not between the values of 5 to 50 mg, the whole procedure was repeated increasing or decreasing the volume of the sample. Suspended solids were calculated as:

$$SS = \frac{F_f - F}{V} \quad (1)$$

where  $SS$  are the suspended solids ( $\text{mg l}^{-1}$ ),  $F$  is the glass microfiber weight before being filtered (mg),  $F_f$  is the glass microfiber filter weight after being filtered (mg) and  $V$  is the volume of the sample (l).

Turbidity and suspended solids were statistically adjusted and it was found that turbidity variability was responsible for 93.02 % of suspended solids variability. Residual plots had no structure, which reflected the goodness of the adjustment. The equation that related suspended solids from turbidity with a regression coefficient  $R^2=0.93$  and  $p < 0.01$  was:

$$SS = 1.5332 \times \text{Turbidity} \quad (2)$$

where  $SS$  are the suspended solids ( $\text{mg l}^{-1}$ ), and turbidity is expressed in FNU.

On the other hand, the amount of retained mass for each filtration cycle was calculated as:

$$R_m = (SS_i - SS_o) \times V_f \quad (3)$$

where  $R_m$  is the retained mass in a filtration cycle (g),  $SS_i$  and  $SS_o$  are the suspended solids at filter inlet and outlet ( $\text{mg l}^{-1}$ ) during a filtration cycle, and  $V_f$  the filtered volume in a filtration cycle ( $\text{m}^3$ ).

### 2.3. Characterisation of inlet reclaimed effluent

The main inlet reclaimed effluent quality parameters for each filter were recorded every minute, as was explained in Section 2.1. Since the filters did not operate simultaneously, it was necessary to assess if effluent characteristics were different during the experiment. Table 2 presents the mean values of the electrical conductivity, dissolved oxygen, pH, temperature, and turbidity values recorded through the 250 hours the experiment lasted for each operating condition.

\*\*\* Table 2 \*\*\*

No significant differences ( $p > 0.05$ ) were found in inlet water quality in any parameter for the three different filter underdrain designs under  $0.20 \text{ m}/30 \text{ m h}^{-1}$  and  $0.30 \text{ m}/60 \text{ m h}^{-1}$  conditions, except for temperature under  $0.30 \text{ m}/60 \text{ m h}^{-1}$ , where the filter with porous media underdrain worked at significantly higher temperatures ( $21.46 \text{ }^\circ\text{C}$ ) than the arm collector underdrain filter ( $19.37 \text{ }^\circ\text{C}$ ). For  $0.30 \text{ m}/30 \text{ m h}^{-1}$ , there were also no differences in temperature.

Under  $0.20 \text{ m}/60 \text{ m h}^{-1}$ , water electrical conductivity inlet values were significantly ( $p < 0.05$ ) lower for the domes underdrain filter ( $2.18 \text{ dS m}^{-1}$ ) than for porous media and arm collector underdrain filters ( $2.79$  and  $2.54 \text{ dS m}^{-1}$ , respectively); dissolved oxygen values for the domes underdrain were significantly higher ( $4.27 \text{ mg l}^{-1}$ ) than with porous media underdrain ( $3.44 \text{ mg l}^{-1}$ ) but not than arm collector underdrain ( $3.93 \text{ mg l}^{-1}$ ); pH for domes underdrain filter ( $7.71$ )

was significantly different from the other two filters, and pH for arm collector filter was also significantly different (7.52) from the porous media underdrain filter (7.29). Water temperature for domes and arm collector underdrain filters were significantly higher (24.01 and 25.02°C, respectively) than that used with porous media underdrain filter (21.03°C), but turbidity values were significantly lower in these two filters (2.84 and 3.50 FNU, respectively) than for the porous media underdrain filter (5.82 FNU).

With 0.30 m/30 m h<sup>-1</sup>, water electrical conductivity inlet values were significantly (p<0.05) lower for the experiments carried out with the porous media underdrain filter (1.85 dS m<sup>-1</sup>) than those with domes and arm collector underdrain filters (2.35 and 2.66 dS m<sup>-1</sup>, respectively). No differences were found in dissolved oxygen values between porous media and domes underdrains and domes and arm collector underdrains, although porous media had significantly higher values (3.37 mg l<sup>-1</sup>) than arm collector underdrain (1.97 mg l<sup>-1</sup>); pH was significantly higher for porous media underdrain (7.71) than with the other two designs. Finally, no significant differences were found among turbidity levels between porous media underdrain and arm collector underdrain, and between arm collector and domes underdrain, but turbidity levels were significantly higher for domes underdrain (7.35 FNU) than for porous media underdrain (4.07 FNU).

Overall, inlet water quality displayed no significant differences when operated at 0.20 m/30 m h<sup>-1</sup> and 0.30 m/60 m h<sup>-1</sup>, but there were different mean groupings for the different monitored quality parameters. This was due to the usual variability found in the composition of reclaimed effluents (Puig-Bargués et al., 2005).

## 2.4. Data treatment and statistical analyses

Filter run time, filtration and backwashing flow, filtration and water backwashing volume, filter pressure at filter inlet and outlet, inlet and outlet reclaimed effluent parameters, filtration and backwashing energy consumption and chlorine injection were recorded every minute by a SCADA system previously developed (Duran-Ros et al., 2008) that was then adapted to this experiment.

Filter performance for removing turbidity and dissolved oxygen was assessed through the removal efficiency (E) achieved in the filters, which was calculated as:

$$E = \frac{N_i - N_o}{N_i} \times 100 \quad (4)$$

where  $N_i$  and  $N_o$  are the values of turbidity and dissolved oxygen at filter inlet and outlet, respectively.

The volume filtered per electrical energy consumption unit,  $V_{eec}$  (m<sup>3</sup> kW h<sup>-1</sup>), was calculated as:

$$V_{eec} = \frac{V_f}{EE_f + EE_b} \quad (5)$$

where  $V_f$  is the filtered volume in a filtration cycle (m<sup>3</sup>), and  $EE_f$  and  $EE_b$  were the electrical energy consumed during a filtration cycle and its backwashing, respectively (kWh).

The time elapsed for a filtration cycle started from the end of a backwashing to the beginning of the following backwashing, if the filter operated in filtration mode between these backwashes. Not all the filtration cycles were taken into account for data treatment. Specifically, those cycles were discarded which did not reach a 50 kPa head loss or those for

which some recorded data were not valid for the whole cycle (e.g. due to maintenance, calibrating processes, scaled down sensors, lower nominal filtration flow or forced backwashing issues). Cycles with inefficient backwashing were also not computed for statistical treatment, as they cannot release most of the particles retained (Duran-Ros et al., 2009b) and tend to accumulate aggregates of the suspended matter, which has a negative impact on filtrate turbidity and on filter run time (Cleasby, 1990). Inefficient backwashes were identified as those with head loss thresholds across the filter greater than 40 kPa after being backwashed. The total number of valid cycles, their total experimental time and the average cycle duration are shown in Table 3.

\*\*\* Table 3 \*\*\*

Statistical analyses were carried out using SPSS Statistics 25 software (IBM, New York, USA). For each parameter, the model that was used included as fixed effects the filter underdrain design, media height and filtration velocity. As the inlet reclaimed effluent parameters were not homogeneous (Table 2), inlet turbidity was taken as a covariate in the model when it was significant, as oxygen was taken dissolved as a covariate in the statistical treatment of dissolved oxygen removal. To differentiate the averages that were significantly different with a probability of 0.05 or less, Tukey's pairwise comparison test was used.

### 3. Results and discussion

#### 3.1. Volume and energy consumption characterization

Table 4 shows the average volumes, electrical energy consumption and retained mass per cycle.

\*\*\* Table 4 \*\*\*

Volumes and electrical energy consumptions depended on operational conditions. Conversely to 0.30 m height, filtered volumes were higher at 60 m h<sup>-1</sup> with 0.20 m. On average, with 0.30 m/60 m h<sup>-1</sup> there were more filtration cycles but they were shorter (Table 3). The lowest filtered volume and electricity consumption were with 0.20 m/30 m h<sup>-1</sup>. Backwashing volumes and their electrical energy consumed were higher at 60 m h<sup>-1</sup> than at 30 m h<sup>-1</sup>, as backwashed nominal flow was higher (Section 2.2), but no significant differences were observed during backwashing periods within the same filtration velocity. In general, more volume was filtered per energy unit at media heights of 0.20 m (8.35 - 8.70 m<sup>3</sup> kWh<sup>-1</sup>) than at 0.30 m (7.67 - 8.22 m<sup>3</sup> kWh<sup>-1</sup>), except for porous media underdrain design at 30 m h<sup>-1</sup>, which filtered 8.50 m<sup>3</sup> kWh<sup>-1</sup>. Overall, porous media underdrain presented the highest values of filtered volume per total electrical energy consumption, with the only exception of 0.20 m/60 m h<sup>-1</sup>. Average values obtained were higher than those (5.26-6.25 m<sup>3</sup> kWh<sup>-1</sup>) found by Soto-García et al. (2013) at farm level (i.e. with higher crop area) in south-eastern Spain. Finally, filter with porous media underdrain retained more mass per cycle than the other two filters in all conditions, except for 0.30 m/30 m h<sup>-1</sup>, when a mass release was observed. In this case, low inlet turbidity values (4.07 FNU) may explain the poor performance of porous media underdrain. Altogether, under the same media heights, lower filtration velocities retained more mass.

## 3.2. Effect of underdrain design and operational conditions on effluent quality

Dissolved oxygen and turbidity removal efficiencies were calculated using Eq. (4), and retained mass using Eq. (3), and their values were statistically treated as was explained in Section 2.4. Table 5 shows the significance level of the model, fixed factors (underdrain design, media height and filtration velocity) and their interactions. Each interaction will be analysed and discussed in the following sub-sections.

\*\*\* Table 5 \*\*\*

### 3.2.1. Dissolved oxygen removal

For the dissolved oxygen (DO) removal efficiency, there was a significant effect ( $p < 0.01$ ) on the underdrain design, with the domes design being the one which increased DO (26.75%) more than porous media and arm collector (11.20 and 11.03 %, respectively). Media height of 0.30 m also increased significantly DO at filter outlet (28.33 %) than 0.20 m (4.30%). In addition, filtration velocity of 30 m h<sup>-1</sup> increased more DO (21.53%) than 60 m h<sup>-1</sup> (15.06 %).

Only the interaction between underdrain design and filtration velocity was significant ( $p < 0.05$ ) for DO removal (Fig. 3). Although under a velocity of 30 m h<sup>-1</sup> there were no significant differences among underdrains, the arm collector design presented higher DO increases (28.01%) followed by the domes (18.21%) and porous media (11.08%) underdrains. Conversely, at 60 m h<sup>-1</sup> the DO increase at filter outlet was significantly higher for the domes (31.10%) than for porous media (11.22%) and arm collector (-3.52%). For the porous media and domes, there was a significant effect ( $p < 0.05$ ) of velocities, with a higher DO increment at 60 m h<sup>-1</sup>. On the contrary, although it was not significant, there was a 112.56% decrease for DO removal efficiency when increasing the velocity from 30 up to 60 m h<sup>-1</sup> with the arm collector filter. DO removals were higher than those observed by Duran-Ros et al. (2009a) (0.49% for 2.80 mg l<sup>-1</sup> inlet DO and  $d_e$  of 0.40 mm) and Elbana et al. (2012) (3.75% for 4.00 mg l<sup>-1</sup> inlet DO and  $d_e$  of 0.48 mm), which were obtained in experiments without any chlorination treatment. The main reason for this DO increase was related to chlorination of backwashing water which reduced microbial population (Li, Chen, Li, Yin, Zhang, 2010) that consumes oxygen. Greater DO increases observed at higher filtration velocities can be attributed to more frequent backwashing (Elbana et al., 2012) as cycles were shorter (Table 3). The higher backwashing flow used at 60 m h<sup>-1</sup> (see Section 2.2), should increase chlorine contact with sand media, reducing microbial population and thus increasing DO. However, performance of arm collector underdrain filter did not follow this pattern as it had fewer backwashing cycles at 60 m h<sup>-1</sup> (113 vs. 152 of porous media underdrain and 153 of domes underdrain).

\*\*\* Figure 3 \*\*\*

### 3.2.2. Turbidity removal and retained mass

For turbidity removal efficiency, there was a significant effect ( $p < 0.05$ ) of the underdrain design, having the porous media the highest removal (26.28%) followed by domes and arm collector (18.53 and 13.45%, respectively). Filtration velocity was also significant, with higher values at 30 m h<sup>-1</sup> (34.17%) than at 60 m h<sup>-1</sup> (11.27%).

The triple interaction of underdrain design, media height and filtration velocity was significant ( $p < 0.05$ ). Thus, interactions between media height and filtration velocity were studied among each underdrain design (Fig. 4). For the porous media, a velocity of  $60 \text{ m h}^{-1}$  significantly ( $p < 0.05$ ) reduced less turbidity than  $30 \text{ m h}^{-1}$  for both media heights of  $0.20 \text{ m}$  (33.63 vs. 38.53%) and  $0.30 \text{ m}$  (14.82 vs. 39.19%). However, turbidity removals were significantly greater with  $0.30 \text{ m}$  at  $30 \text{ m h}^{-1}$  and with  $0.20 \text{ m}$  at  $60 \text{ m h}^{-1}$ . With this last velocity, differences in turbidity removal were more pronounced (33.63% with  $0.20 \text{ m}$  versus 14.82% with  $0.30 \text{ m}$ ).

For the dome underdrain, with a porous media height of  $0.20 \text{ m}$ ,  $30 \text{ m h}^{-1}$  showed higher turbidity removals (31.91%) than with  $60 \text{ m h}^{-1}$  (1.04%), although they were not significant due to the high dispersion of inlet turbidity values used as a covariate. With a media height of  $0.30 \text{ m}$ ,  $30 \text{ m h}^{-1}$  also achieved significant higher turbidity removals (47.74%) than at  $60 \text{ m h}^{-1}$  (10.51%). On the other hand, the  $0.30 \text{ m}$  media height removed turbidity significantly greater than  $0.20 \text{ m}$  for both  $30 \text{ m h}^{-1}$  (47.74 vs. 31.91%) and  $60 \text{ m h}^{-1}$  (10.51 vs. 1.04%).

A significant ( $p < 0.05$ ) interaction between media height and filtration velocity was also observed for the arm collector design. With both  $0.20$  and  $0.3 \text{ m}$ ,  $30 \text{ m h}^{-1}$  had significant higher turbidity removals (35.89% and 16.04%) than with  $60 \text{ m h}^{-1}$  (-9.93% and 3.30%). Media height effect was also significant between filtration velocities. With  $30 \text{ m h}^{-1}$ ,  $0.20 \text{ m}$  height showed significantly higher turbidity removals (35.89 %) than with  $0.30 \text{ m}$  (16.04 %) but, conversely, with  $60 \text{ m h}^{-1}$ , only the  $0.30 \text{ m}$  media height removed turbidity (3.30 %).

Overall, porous media design presented higher turbidity removals than the other two underdrains in all the operative conditions tested, except for a  $0.30 \text{ m}/30 \text{ m h}^{-1}$ , for which the dome underdrain achieved higher removals (47.74% vs. 39.19%). For all the designs, higher filtration velocities ( $60 \text{ m h}^{-1}$ ) presented less turbidity removals. However, there was not a clear pattern in media height variations.

Higher solid removals were observed at higher velocities when more loaded water was used (de Deus, Testezlaf and Mesquita, 2016; Mesquita et al., 2009a). Moreover, at high filtration velocities, solid removal tend to happen in the first filtration layers, with the media height not being as important as filtration velocity. However, at lower filtration rates, this tendency is not so clear (de Deus et al., 2016), as our results also have shown.

Underdrain design also affects backwashing cleaning process as underdrains are essential to guarantee an homogeneous particle removal and reduced head loss during backwashing (Mesquita, 2014). The analysis of backwashing flow depending on the design was not studied in the present paper, but further research is warranted since it is a key factor in filter performance.

\*\*\* Figure 4 \*\*\*

The small inlet levels of turbidity of the reclaimed effluent and the small media height bed used in the filters may also explain the small turbidity removals obtained. The media height bed used in the present experiment (see Section 2.2) was between 40 and 60% lower than the heights used by Duran-Ros et al. (2009a) and Elbana et al. (2012). These authors, with similar effluents to those of the present experiment, observed turbidity removals that ranged 57-66%, using sands with  $d_e$  of  $0.27 - 0.40 \text{ mm}$  and  $UC_s$  of  $1.81 - 2.89$  and inlet turbidity of  $4.08 - 10.80$

FNU. Wu et al. (2015) used similar grain sand sizes obtaining total suspended solid removal efficiencies of 34 and 48 % with  $d_e$  of 0.45 and 0.41 mm and  $UC_s$  of 2.04 and 1.95, respectively. On the other hand, Tripathi, Rajput and Patel (2014) obtained turbidity reductions of 51% using effluents with inlet 55 FNU. However, in neither of the two other papers were details of the sand filter design and media heights provided.

For the calculated retained mass per cycle (Table 5) there was a significant effect ( $p < 0.001$ ) of the underdrain and media height, being the porous media the design which retained more mass ( $81.78 \text{ g cycle}^{-1}$ ), followed by the dome ( $50.11 \text{ g cycle}^{-1}$ ) and arm collector ( $39.38 \text{ g cycle}^{-1}$ ). In addition, the height of 0.20 m retained greater mass ( $78.67 \text{ g cycle}^{-1}$ ) than 0.30 m ( $41.47 \text{ g cycle}^{-1}$ ) ( $p < 0.05$ ). The triple interaction of underdrain, media height and filtration velocity was also significant and followed the same pattern as in turbidity removal explained above, as total suspended solid is highly correlated with turbidity (Eq. (2)). The effect of underdrain design on retained mass has been previously reported by Burt (2010), who, conversely to our results, found that an arm collector underdrain, which was different from that used in the present study, retained more mass than a screen-domes underdrain. These results highlight the importance of filter design on its performance.

### 3.3. Effect of filter and operational conditions on water and energy consumption

Filtered volume and filtered water volume per electrical energy consumption unit were also statistically analysed (Table 6). In the following sub-sections, significant interactions for each parameter will be discussed.

\*\*\* Table 6 \*\*\*

#### 3.3.1. Filtered volume per filtration cycle

There was a significant effect ( $p < 0.001$ ) of underdrain and media height on the filtered volume. On average, porous media filtered more volume per cycle ( $38.41 \text{ m}^3$ ), followed by the arm collector ( $33.69 \text{ m}^3$ ) and dome ( $31.73 \text{ m}^3$ ); while with 0.20 m more effluent was filtered ( $36.42 \text{ m}^3$ ) than under 0.30 m ( $32.97 \text{ m}^3$ ). Double interactions between underdrain and media height, media height and filtration velocity, and underdrain design and filtration velocity were all significant (Table 6).

With a height of 0.20 m, no significant differences among underdrains were found (Fig. 5), but at 0.30 m, the porous media underdrain filtered significantly more ( $p < 0.05$ ) volume ( $39.35 \text{ m}^3$ ) than the dome ( $28.01 \text{ m}^3$ ), but without significant differences with the arm collector ( $34.61 \text{ m}^3$ ). However, for each filter there were no significant differences in filtered volume between both media heights.

The height of 0.20 m (Fig. 6) yielded more filtered volume ( $p < 0.05$ ) at  $60 \text{ m h}^{-1}$  ( $49.23 \text{ m}^3$ ) than at  $30 \text{ m h}^{-1}$  ( $18.75 \text{ m}^3$ ), which appears to be logical because higher filtration velocity was achieved by higher nominal flow. But at 0.30 m, the filtered volume was significantly higher at  $30 \text{ m h}^{-1}$  ( $45.13 \text{ m}^3$ ) than at  $60 \text{ m h}^{-1}$  ( $29.57 \text{ m}^3$ ). This fact could be explained for the low inlet turbidity values obtained when the porous media was tested at  $0.30 \text{ m}/30 \text{ m h}^{-1}$  (Table 2), with consequent longer filtration cycles, increasing thus the filtered volume for all the filters, while

at 60 m h<sup>-1</sup> the pressure loss produced across the filter quickly reached the pre-set threshold of 50 kPa, where backwashing was activated.

The porous media design filtered significantly more water at 30 m h<sup>-1</sup> (54.94 m<sup>3</sup>) than the dome and arm collector (30.20 and 24.48 m<sup>3</sup>, respectively) probably due to the cleaner effluent produced in the WWTP during its use, but at 60 m h<sup>-1</sup> both porous media and arm collector filtered significantly more water (35.55 and 40.66 m<sup>3</sup>, respectively) than the dome design (32.36 m<sup>3</sup>). All the underdrains presented significant differences of filtered water volume between velocities. However, porous media underdrain filtered more volume at 30 m h<sup>-1</sup> (54.94 m<sup>3</sup>) than at 60 m h<sup>-1</sup> (35.55 m<sup>3</sup>). Conversely, domes and arm collector filtered more water at 60 m h<sup>-1</sup> (32.36 m<sup>3</sup> and 40.66 m<sup>3</sup>, respectively) than at 30 m h<sup>-1</sup> (30.20 and 24.48 m<sup>3</sup>, respectively) (Fig. 7).

\*\*\* Figures 5, 6 and 7 \*\*\*

### 3.3.2. Filtered volume per total electrical consumption

The ratio between filtered volume and total electrical energy consumption (i.e. considering both filtration and backwashing), which was calculated with Eq. (5), significantly ( $p < 0.05$ ) depended on underdrain, media height and filtration velocity (Table 6). The porous media design filtered more water volume per kWh consumed, followed by the domes and arm collector (8.30, 8.18 and 8.07 m<sup>3</sup> kW h<sup>-1</sup>, respectively). The height of 0.20 m had higher ratios than 0.30 m (8.53 vs. 7.95 m<sup>3</sup> kW h<sup>-1</sup>) as well as velocity of 30 m h<sup>-1</sup> regarding 60 m h<sup>-1</sup> (8.35 vs. 8.11 m<sup>3</sup> kW h<sup>-1</sup>). Interactions between media height and filtration velocities as well as between underdrain designs and filtration velocities were found to be significant.

There were no significant differences between filtration velocities at 0.20 m (Fig. 8), with similar values at 60 m h<sup>-1</sup> and 30 m h<sup>-1</sup> (8.57 and 8.47 m<sup>3</sup> kW h<sup>-1</sup>, respectively). However, with a height of 0.30 m, this ratio was significantly higher at 30 m h<sup>-1</sup> than at 60 m h<sup>-1</sup> (8.21 vs. 7.87 m<sup>3</sup> kW h<sup>-1</sup>). As was previously discussed in Section 3.3.1, higher ratios at 30 m h<sup>-1</sup> than at 60 m h<sup>-1</sup> with 0.30 m height could be explained by the longer filtration cycles of porous media underdrain at 0.30 m/30 m h<sup>-1</sup> due to the occasional lower inlet turbidity. On the other hand, at 60 m h<sup>-1</sup> a faster pressure loss was produced due to higher velocity, with the consequent shorter filtration cycles and less filtered volume. In that sense, for all the designs, higher ratio values were obtained at 30 m h<sup>-1</sup> than at 60 m h<sup>-1</sup>, although nominal flow was higher at 60 m h<sup>-1</sup>. The ratio was higher with a height of 0.20 than 0.30 m, as there was more flow resistance due to a greater sand bed thickness in the latter.

At 30 m h<sup>-1</sup>, porous media underdrain presented a significantly ( $p < 0.05$ ) higher ratio (8.61 m<sup>3</sup> kW h<sup>-1</sup>) than arm collector and domes (8.33 and 8.27 m<sup>3</sup> kW h<sup>-1</sup>, respectively), but at 60 m h<sup>-1</sup>, both porous media and dome designs (Fig. 9) showed greater ratios (8.25 and 8.14 m<sup>3</sup> kW h<sup>-1</sup>, respectively) than arm collector (7.88 m<sup>3</sup> kW h<sup>-1</sup>).

Results for volume and electrical energy consumption concur with those obtained by Mesquita et al. (2012), in which the effect of three sand filters with different designs on head loss was tested using clean water and different sand sizes, media heights and filtration velocities, being all the factors and their interactions significant. Head loss increased proportionally with filtration velocity (Burt, 2010; Mesquita et al., 2012) as well as with deeper sand heights

(Mesquita et al., 2012). However, at a low filtration velocity of  $20 \text{ m h}^{-1}$ , no significant differences were detected with different heights. Two of the underdrains tested by Mesquita et al. (2012) were similar to those used in the present experiment (arm collector and domes) and the former presented higher pressure losses than the latter in almost all conditions tested. Nevertheless, Burt (2010), studying two similar designs (arm collector and dome), did not find that a specific design had a more significant effect in pressure loss.

\*\*\* Figures 8 and 9 \*\*\*

## 4. Conclusions

Media height, filtration velocity and the underdrain design affected removal efficiency, filtered volume and electrical energy consumption of sand filters for microirrigation systems using reclaimed effluents in field conditions.

Overall, when using reclaimed effluents with similar characteristics as this experiment in sand media filters, working at a filtration velocity of  $30 \text{ m h}^{-1}$  instead of  $60 \text{ m h}^{-1}$  provide higher turbidity removals (34.17 vs. 11.27%), higher mass retention ( $84.97$  vs.  $31.56 \text{ g cycle}^{-1}$ ), longer filtration cycles (289 vs. 178 min) and higher ratio of filtered volume per electrical energy unit ( $8.35$  vs.  $8.11 \text{ m}^3 \text{ kW h}^{-1}$ ).

On the other hand, a porous media underdrain that improves hydraulic performance of the sand media achieved better turbidity removals (26.28% vs. 18.53 and 13.45% of the domes and arm collector underdrains, respectively), more filtered volume per filtration cycle ( $38.41$  vs.  $31.73$  and  $33.69 \text{ m}^3$ ) and more filtered volume per electrical consumption ratio ( $8.30$  vs.  $8.18$  and  $8.07 \text{ m}^3 \text{ kW h}^{-1}$ ) than the other two underdrain designs tested under the same operational conditions. The porous media underdrain removes 12.83% more of turbidity with 2.77% less energy consumption regarding the filter that showed the lowest values.

Media height, however, did not follow a clear pattern either in turbidity removal or in filtered volume. As with a 0.20 m lower media height, higher filtered volume per electrical energy unit ratio was observed, thus lower media heights are recommended, considering that additional savings for the smaller amount of media required would be achieved.

Further research is needed for confirming the results with other effluents, media heights, filtration velocities and underdrain designs. The effect of the factors here considered in backwashing efficiency requires also new specific studies.

## 5. Acknowledgements

The authors would like to express their gratitude to the former Spanish Ministry of Economy and Competiveness for its financial support for this experiment through grant AGL2015-63750-R. Carles Solé Torres was the recipient of a predoctoral scholarship (IFUdG2016/72) from the University of Girona. The authors would also like to thank the Municipality of Celrà for their help in carrying out this experiment.

## 6. References

- Abadía, R., Vera, J., Rocamora, C., & Puerto, H. (2018). Generalization of supply energy efficiency in irrigation distribution networks. *Biosystems Engineering*, 175, 146-155.
- Arbat, G., Pujol, T., Puig-Bargués, J., Duran-Ros, M., Barragán, J., Montoro, L., & Ramírez de Cartagena, F. (2011). Using computational fluid dynamics to predict head losses in the auxiliary elements of a microirrigation sand filter. *Transactions of the ASABE*, 54(4), 1367-1376.
- Asano, T., Burton, F.L., & Leverenz, H.L. (2007). Water reuse: issues, technologies and applications. New York, USA: McGraw Hill Inc.
- Bové, J., Arbat, G., Pujol, T., Duran-Ros, M., Ramírez de Cartagena, F., Velayos, J., & Puig-Bargués, J. (2015a). Reducing energy requirements for sand filtration in microirrigation: improving the underdrain and packing. *Biosystems Engineering*, 140, 67–78.
- Bové, J., Arbat, G., Duran-Ros, M., Pujol, T., Velayos, J., Ramírez de Cartagena, F. & Puig-Bargués, J. (2015b). Pressure drop across sand and recycled glass media used in micro irrigation filters. *Biosystems Engineering*, 137, 55 - 63.
- Bové, J., Puig-Bargués, J., Arbat, G., Duran-Ros, M., Pujol, T., Pujol, J., & Ramírez de Cartagena, F. (2017). Development of a new underdrain for improving the efficiency of microirrigation sand media filters. *Agricultural Water Management*, 179, 296-305.
- Bové, J.; Pujol, J.; Arbat, G.; Duran-Ros, M.; Ramírez de Cartagena, F.; & Puig-Bargués, J. (2018). Environmental assessment of underdrain designs for a sand media filter. *Biosystems Engineering*, 167, 126-136.
- Burt, C. (2010). Hydraulics of commercial sand media filter tank used for agricultural drip irrigation. ITCR Report No. R 10001. San Luis Obispo, CA, USA: Irrigation Training and Research Center.
- Burt, C., Howes, D. J., & Freeman, B. (2011). Public Interest Energy Research (PIER) Program. Final Project Report, Agriculture Water Energy Efficiency (p. 263). San Luis Obispo, CA, USA: California Energy Commission and Irrigation Training and Research Center.
- Capra, A., & Scicolone, B. (2007). Recycling of poor quality urban wastewater by drip irrigation systems. *Journal of Cleaner Production*, 15 (16), 1529–1534.
- Cleasby, J.L. (1990). Filtration. In: American Water Work Association Water quality and Treatment: A Handbook of Public Water Supplies, Fourth ed. New York, USA: McGraw-Hill, Inc.
- De Deus, FP., Testezlaf, R., & Mesquita, M. (2016). Assessment methodology of backwashing in pressurized sand filters. *Revista Brasileira de Engenharia Agrícola e Ambiental*, 20 (7), 600-605.
- Duran-Ros, M., Puig-Bargués, J., Arbat, G., Barragán, J., & Ramírez de Cartagena, F. (2008). Definition of a SCADA system for a microirrigation network with effluents. *Computers and Electronics in Agriculture*, 64 (2), 338-342.

- Duran-Ros, M., Puig-Bargués, J., Arbat, G., Barragán, J., & Ramírez de Cartagena, F. (2009a). Effect of filter, emitter and location on clogging when using effluents. *Agricultural Water Management*, 96 (10), 67–79.
- Duran-Ros, M., Puig-Bargués, J., Arbat, G., Barragán, J., & Ramírez de Cartagena, F. (2009b). Performance and backwashing efficiency of disc and screen filters in microirrigation systems. *Biosystems Engineering*, 103(1), 35-42.
- Duran-Ros, M., Arbat, G., Barragán, J., Ramírez de Cartagena, F., & Puig-Bargués, J. (2010). Assessment of head loss equations developed with dimensional analysis for micro irrigation filters using effluents. *Biosystems Engineering*, 106, 521–526.
- Elbana, M., Ramírez de Cartagena, J., & Puig-Bargués, J. (2012). Effectiveness of sand media filters for removing turbidity and recovering dissolved oxygen from a reclaimed effluent used for micro-irrigation. *Agricultural Water Management*, 111, 27-33.
- Elbana, M., Ramírez de Cartagena, J., & Puig-Bargués, J. (2013). New mathematical model for computing head loss across sand media filter for microirrigation systems. *Irrigation Science*, 31, 343 – 349.
- Fernández García, I., Montesinos, P., Camacho Poyato, E., & Rodríguez Díaz, J.A. (2017). Optimal design of pressurized irrigation networks to minimize the operational cost under different management scenarios. *Water Resources Management*, 31(6), 1995-2010.
- Li, J., Chen, L., Li, Y., Yin, J., & Zhang, H. (2010). Effects of chlorination schemes on clogging in drip emitters during application of sewage effluent. *Applied Engineering in Agriculture*. 26(4), 565–578.
- Jiménez-Bello, M.A., Royuela, A., Manzano, J., García Prats, A., & Martínez-Alzamora, F. (2015). Methodology to improve water and energy use by proper irrigation scheduling in pressurized networks. *Agricultural Water Management*, 149, 91-101.
- Mesquita, M. (2014). *Desenvolvimento tecnológico de um filtro de areia para irrigação localizada* (Unpublished doctoral dissertation). Universidade Estadual de Campinas, Campinas, Brazil.
- Mesquita, M., Testezlaf, R., & Ramirez, J. (2012). The effect of media bed characteristics and internal auxiliary elements on sand filter head loss. *Agricultural Water Management*, 115, 178-185.
- Mesquita, M., de Deus, F.P., Testezlaf, R., & Diotto, A.V. (2019a). Removal efficiency of pressurized sand filters during the filtration process. *Desalination and Water Treatment*, 161, 132-143.
- Mesquita, M., de Deus, F.P., Testezlaf, R., da Rosa, L.M., & Diotto, A.V. (2019b). Design and hydrodynamic performance testing of a new pressure sand filter diffuser plate using numerical simulation. *Biosystems Engineering*, 183, 58-69.

- Moreno, M.A., del Castillo, A., Montero, J., Tarjuelo, J.M., & Ballesteros, R. (2016). Optimization of the design of pressurized irrigation systems for irregular shaped plots. *Biosystems Engineering*, 151, 361-373.
- Nakayama, F.S., Boman, B.J., & Pitts, D.J. (2007). Maintenance. In: F.R. Lamm, J.E Ayars, & F.S. Nakayama, F.S. (Eds.), *Microirrigation for Crop Production. Design, Operation, and Management* (pp. 389-430). Amsterdam, Netherlands: Elsevier.
- Nakhla, G., & Farooq, S. (2003). Simultaneous nitrification–denitrification in slow sand filters. *Journal of Hazardous Materials* 96(2–3), 291–303
- Pizarro, F. (1996). *Riegos localizados de alta frecuencia*, 3rd ed. Madrid, Spain: Mundi Prensa.
- Pujol, T., Arbat, G., Bové, J., Puig-Bargués, J., Duran-Ros, M., Velayos, J., & Ramírez de Cartagena, F. (2016). Effects of the underdrain design on the pressure drop in sand filters. *Biosystems Engineering*, 150, 1-9.
- Puig-Bargués, J., Barragán, J., & Ramírez de Cartagena, F. (2005). Filtration of effluents for microirrigation systems. *Transactions of the ASAE*, 48(3): 968–978
- Solé-Torres, C., Puig-Bargués, J. Duran-Ros, M., Arbat, G., Pujol, J., & Ramírez de Cartagena, F. (2019). Effect of different sand filter underdrain designs on emitter clogging using reclaimed effluents. *Agricultural Water Management*, 223, 105683.
- Soto-García, M., Martín-Gorrioz, B., García-Bastida, P.A., Alcón, F.; & Martínez-Álvarez, V. (2013). Energy consumption for crop irrigation in a semiarid climate (south-eastern Spain). *Energy*, 55, 1084-1093.
- Tarjuelo, J.M., Rodríguez-Díaz, J.A., Abadía, R., Camacho, E., Rocamora, C., & Moreno, M.A. (2015). Efficient water and energy use in irrigation modernization: Lessons from Spanish case studies. *Agricultural Water Management*, 162, 67-77.
- Tripathi, V.K., Rajput, T.B.S., & Patel, N. (2014). Performance of different filter combinations with surface and subsurface drip irrigation systems for utilizing municipal wastewater. *Irrigation Science*, 32, 379-391.
- Trooien, T.P., & Hills, D.J. (2007). Application of biological effluent. In: F.R. Lamm, J.E. Ayars, & F.S. Nakayama (Eds.), *Microirrigation for Crop Production. Design, Operation, and Management* (pp. 329-356). Amsterdam, Netherlands: Elsevier (Chapter 9).
- World Health Organization, WHO (2006) *Guidelines for the safe use of wastewater, excreta and greywater*, vol II. Geneva, Switzerland: WHO Press.
- Wu, W.Y., Huang, Y., Liu, H.L., Yin, S.Y., & Niu, Y. (2015). Reclaimed water filtration efficiency and drip irrigation emitter performance with different combinations of sand and disc filters. *Irrigation and Drainage*, 64 (3), 362-369.

## Figures



Fig. 1. Different underdrain designs: porous media (A), inserted domes (B) and arm collector (C).

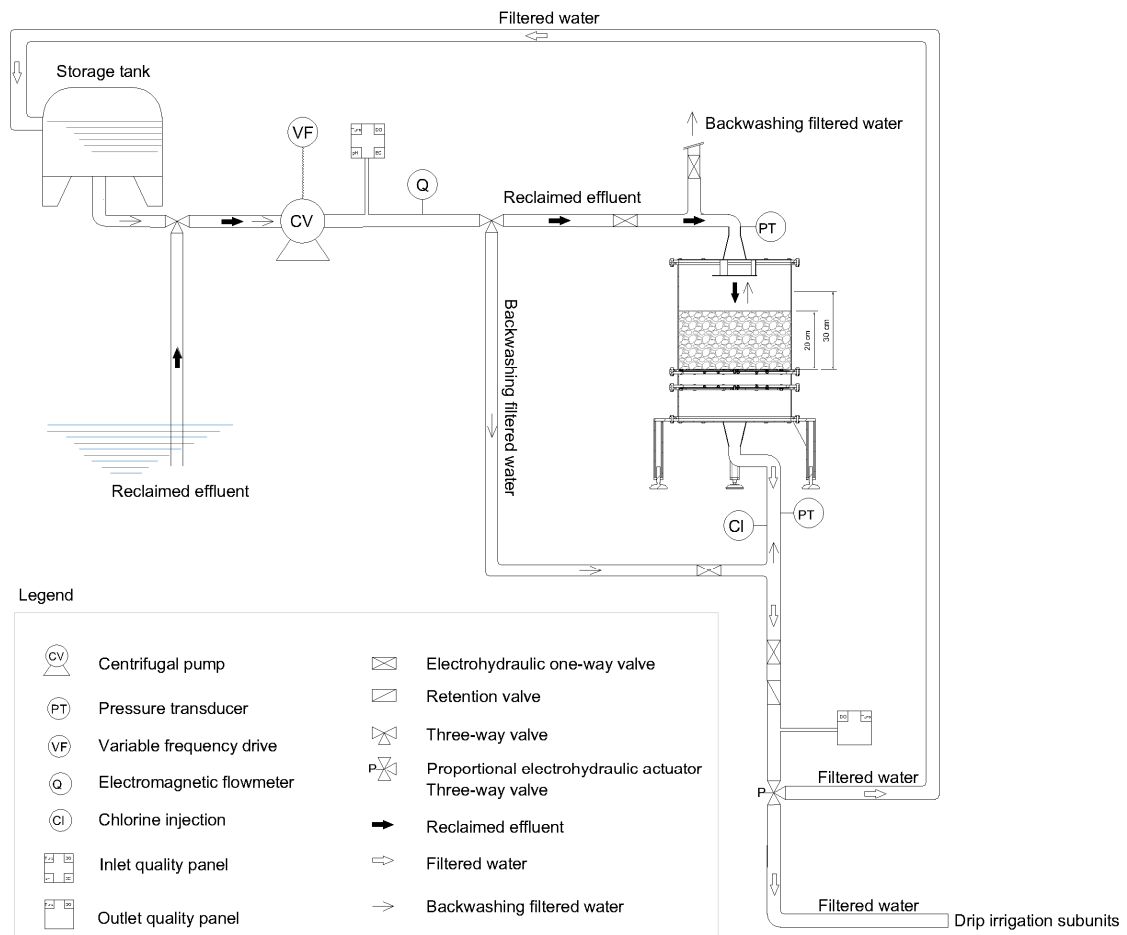


Fig. 2. Diagram of the experimental system. For simplicity, only one of the three filters is depicted.

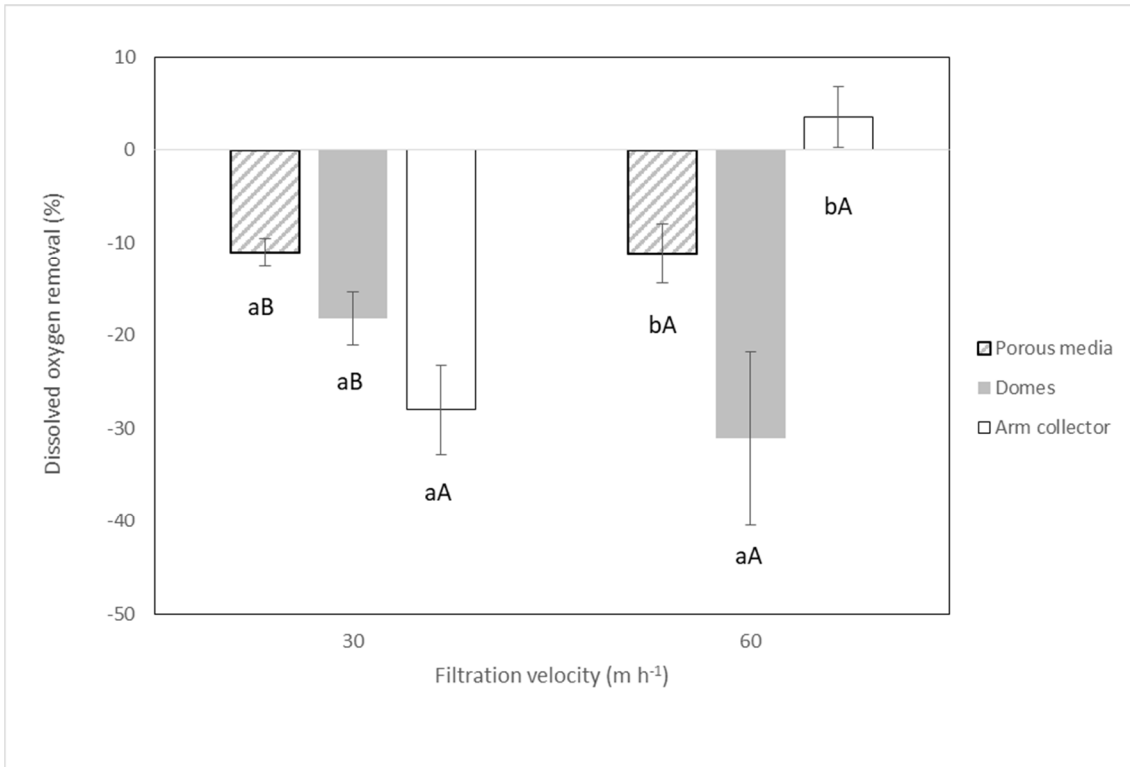


Fig. 3. Dissolved oxygen removal efficiency and standard error bars (%) for the different underdrain designs at the two filtration velocities. For each filtration velocity, different small letters mean significant differences ( $p < 0.05$ ) among underdrain designs. For each underdrain design, capital letters mean significant differences ( $p < 0.05$ ) between filtration velocities.

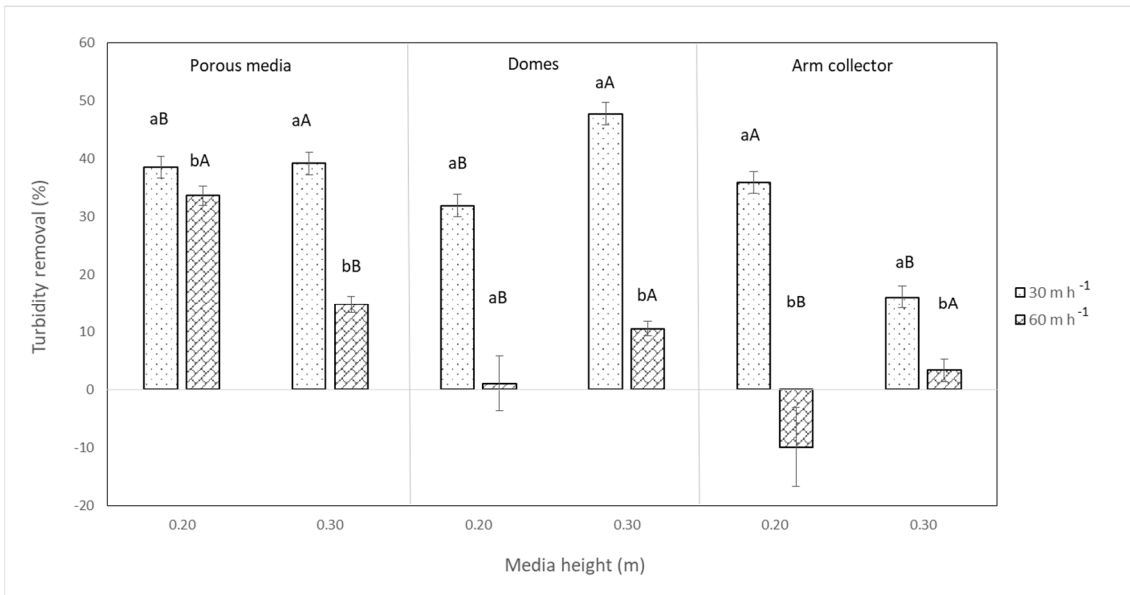


Fig. 4. Interactions between media height and filtration velocity for each underdrain design in turbidity removal efficiency (%). For each media height and underdrain design, small letters mean significant differences ( $p < 0.05$ ) between filtration velocities. For each filtration velocity and underdrain design, different capital letters mean significant differences ( $p < 0.05$ ) between media heights.

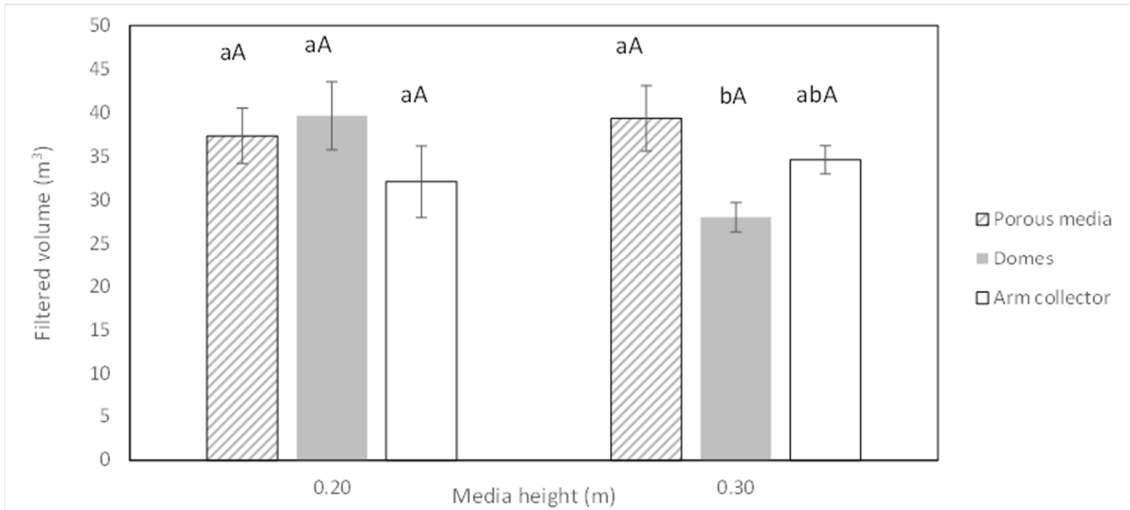


Fig. 5. Interactions between media heights and underdrain designs for filtered water volume per cycle ( $\text{m}^3$ ). For each media height, small letters mean significant differences ( $p < 0.05$ ) among underdrain designs. For each underdrain design, different capital letters mean significant differences ( $p < 0.05$ ) among media heights.

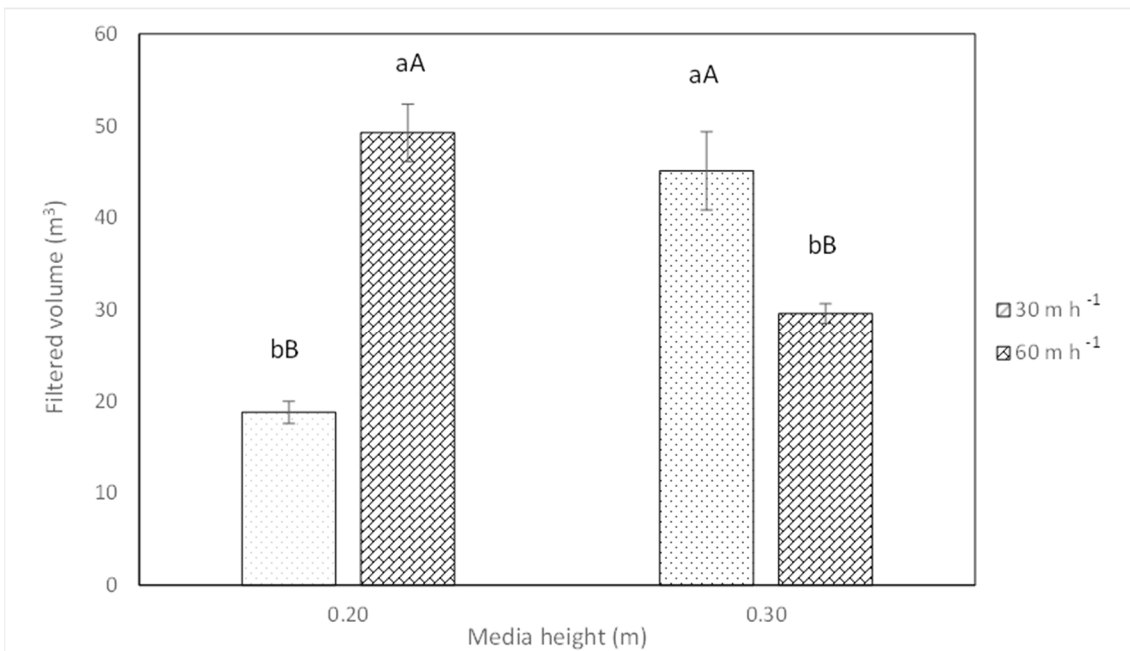


Fig. 6. Interactions between media heights and filtration velocities for filtered water volume per cycle ( $\text{m}^3$ ). For each media height, small letters mean significant differences ( $p < 0.05$ ) between filtration velocities. For each filtration velocity, different capital letters mean significant differences ( $p < 0.05$ ) between media heights.

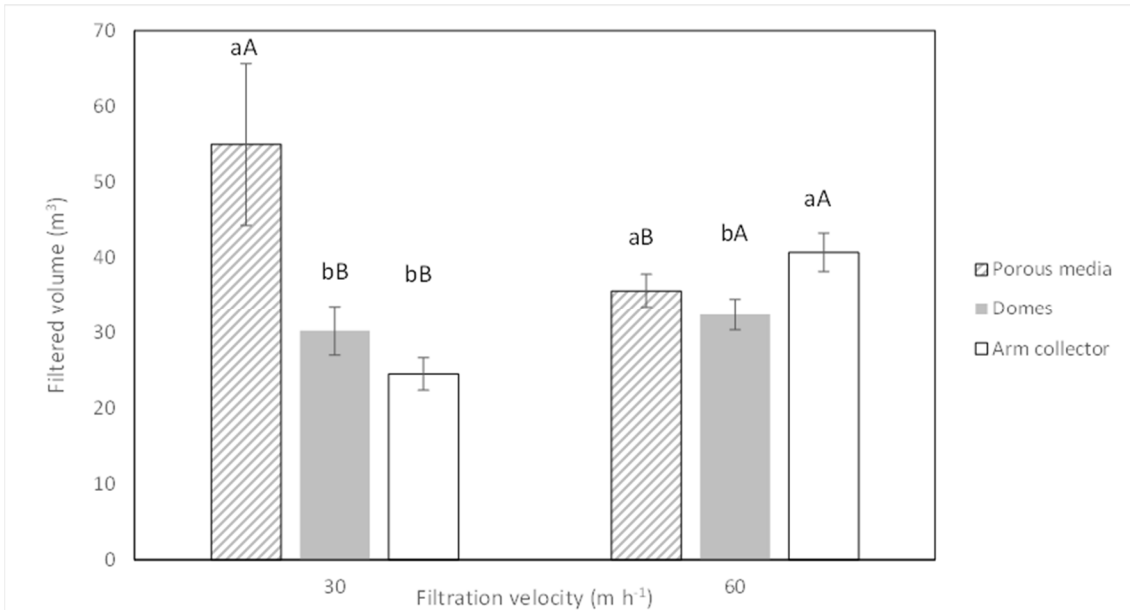


Fig. 7. Interactions between filtration velocities and underdrain designs for filtered water volume per cycle (m<sup>3</sup>). For each filtration velocity, small letters mean significant differences ( $p < 0.05$ ) among underdrain designs. For each underdrain design, different capital letters mean significant differences ( $p < 0.05$ ) between filtration velocity.

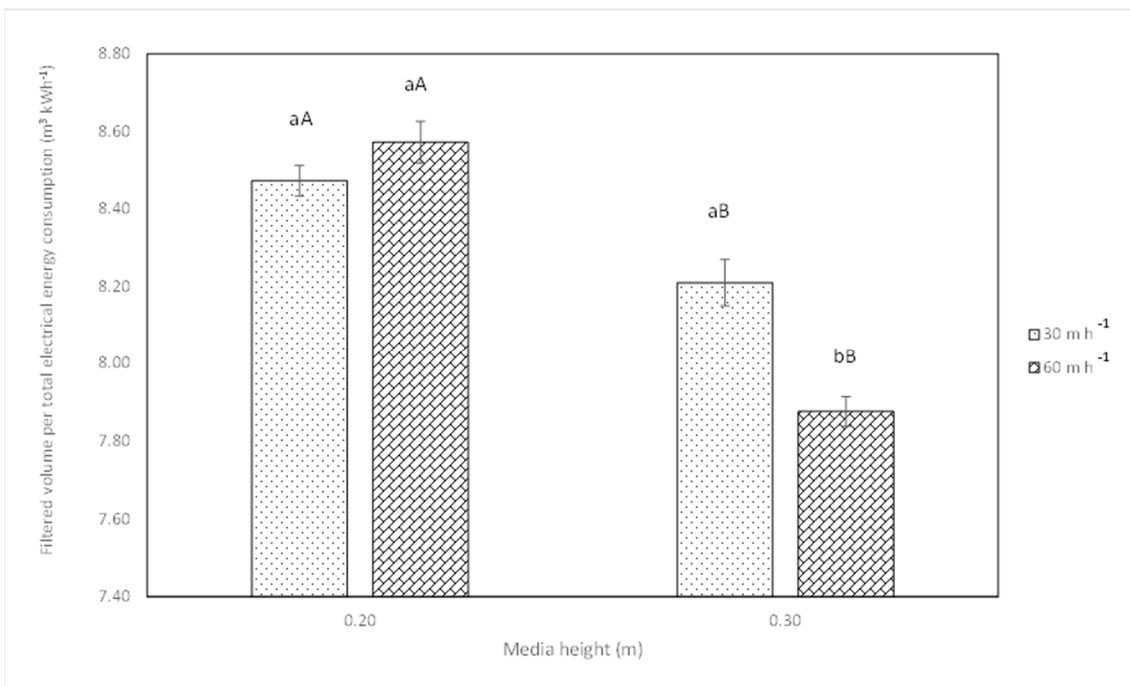


Fig. 8. Interactions between media heights and filtration velocities for filtered water volume per total energy consumption (m<sup>3</sup> kW h<sup>-1</sup>). For each media height, small letters mean significant differences ( $p < 0.05$ ) between filtration velocities. For each filtration velocity, different capital letters mean significant differences ( $p < 0.05$ ) between media heights.

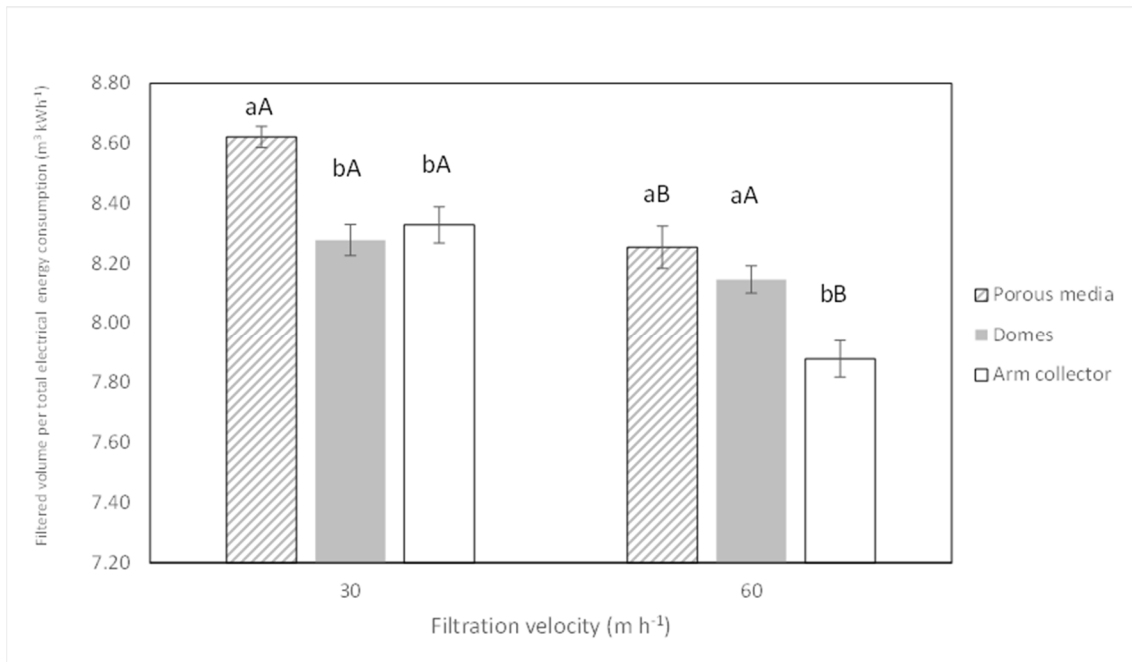


Fig. 9. Interactions between filtration velocity and underdrain design in filtered water volume per total energy consumption ( $\text{m}^3\text{kW h}^{-1}$ ). For each filtration velocity, small letters mean significant differences ( $p < 0.05$ ) among underdrain designs. For each underdrain design, different capital letters mean significant differences ( $p < 0.05$ ) between filtration velocities.

## Tables captions

Table 1. Underdrain design and main operation characteristics of the different filters used in the experiment. Data was obtained from manufacturers.

Characteristic	Filter underdrain design		
	Porous media	Domes	Collector arms
Filter nominal diameter (mm)	500	508	500
Filter filtration surface (m <sup>2</sup> )	0.1960	0.2026	0.1960
Maximum filtration flow (m <sup>3</sup> h <sup>-1</sup> )	20	18	23
Maximum filtration height (m)	0.70	0.69	0.40
Number of underdrains	1	12	10
Mean slot width (m)	-	4.5 x 10 <sup>-4</sup>	2.5 x 10 <sup>-4</sup>
Number of slots by underdrains	-	90	140
Underdrain opening area per underdrain unit (m <sup>2</sup> )	7.44 x 10 <sup>-2</sup>	6.26 x 10 <sup>-4</sup>	9.11 x 10 <sup>-4</sup>
Underdrain total opening area (m <sup>2</sup> )	0.0744	0.0075	0.0091
Underdrain effective area (ratio of underdrain opening area to filter surface area, %)	37.95	3.71	4.65

Table 2. Average ± standard error of the effluent physical and chemical parameters at filter inlets. Different letters mean that there were significant differences (p<0.05) in the values of each parameter at the different filter inlets.

Media height	Filtration velocity	Underdrain design	Electrical conductivity	Dissolved oxygen	pH	Temperature	Turbidity
(m)	(mh <sup>-1</sup> )		(dS m <sup>-1</sup> )	(mg l <sup>-1</sup> )	(-)	(°C)	(FNU)
0.20	30	Porous media	2.68 ±1.24 abc	2.69 ±0.15 def	7.04 ±0.02 f	15.29 ±0.51 g	8.16 ±0.36 ab
		Domes	2.90 ±0.79 a	3.07 ±0.11 cde	7.10 ±0.02 f	15.31 ±0.31 g	7.49 ±0.36 abc
		Arm collector	2.89 ±0.57 a	2.89 ±0.09 def	7.07 ±0.02 f	16.35 ±0.28 g	8.51 ±0.42 a
0.20	60	Porous media	2.79 ±0.40 ab	3.44 ±0.08 bcd	7.29 ±0.02 e	21.03 ±0.40 def	5.82 ±0.21 cd
		Domes	2.18 ±0.71 de	4.27 ±0.11 a	7.71 ±0.02 a	24.01 ±0.21 ab	2.84 ±0.17 e
		Arm collector	2.54 ±0.29 bc	3.93 ±0.16 ab	7.52 ±0.02 b	25.02 ±0.11 a	3.50 ±0.30 e
0.30	30	Porous media	1.85 ±1.49 e	3.37 ±0.28 bcde	7.71 ±0.05 a	22.50 ±0.25 bcd	4.07 ±1.04 de
		Domes	2.35 ±0.62 cd	2.66 ±0.20 ef	7.51 ±0.02 bc	23.17 ±0.11 b	7.35 ±0.91 abc
		Arm collector	2.66 ±0.42 abc	1.97 ±0.14 f	7.42 ±0.01cd	23.11 ±0.08 bc	5.91 ±0.31 cd
0.30	60	Porous media	2.58 ±0.48 abc	3.23 ±0.12 bcde	7.39 ±0.01 de	21.46 ±0.22 cde	6.29 ±0.23 bc
		Domes	2.38 ±0.41 cd	3.45 ±0.13 bcd	7.44 ±0.01 bcd	20.04 ±0.17 ef	5.77 ±0.17 cd
		Arm collector	2.43 ±0.49 cd	3.79 ±0.10 abc	7.38 ±0.01 de	19.37 ±0.27 f	5.98 ±0.24 cd

Table 3. Number of valid cycles and total experimental duration of the different operational condition for each filter and the average  $\pm$  standard error of the cycle durations.

Media height (m)	Filtration velocity (m h <sup>-1</sup> )	Underdrain design	Number of valid cycles	Total duration (h)	Average cycle duration (min)
0.20	30	Porous media	21	94.58	270.24 $\pm$ 35.81
		Domes	55	206.50	229.44 $\pm$ 29.81
		Arm collector	64	241.80	226.69 $\pm$ 31.50
0.20	60	Porous media	77	222.45	180.36 $\pm$ 15.34
		Domes	42	192.28	274.69 $\pm$ 25.83
		Arm collector	29	126.12	260.93 $\pm$ 39.70
0.30	30	Porous media	10	172.45	1034.70 $\pm$ 222.18
		Domes	36	236.30	393.83 $\pm$ 48.02
		Arm collector	35	212.58	364.43 $\pm$ 38.25
0.30	60	Porous media	75	209.47	167.57 $\pm$ 12.77
		Domes	111	226.47	122.41 $\pm$ 6.99
		Arm collector	84	236.63	169.02 $\pm$ 8.05

Table 4. Average  $\pm$  standard error values of the main volume, energy consumption and mass retention for each experimental condition.

Media height (m)	Filtration velocity (m h <sup>-1</sup> )	Underdrain design	Filtered volume per filtration cycle (m <sup>3</sup> )	Backwashing volume per filtration cycle (m <sup>3</sup> )	Backwashing per total volume ratio (%)	Electrical consumption per filtration cycle (kWh)	Electrical consumption per backwashing cycle (kWh)	Backwashing energy consumption ratio (%)	Filtered volume per total electrical consumption (m <sup>3</sup> kWh <sup>-1</sup> )	Retained mass per cycle (g)
0.20	30	Porous media	31.04 $\pm$ 4.84	0.45 $\pm$ 0.003	1.76 $\pm$ 0.27	3.14 $\pm$ 0.41	0.02 $\pm$ 0.001	0.78 $\pm$ 0.11	8.70 $\pm$ 0.04	180.70 $\pm$ 39.97
		Domes	17.51 $\pm$ 1.64	0.45 $\pm$ 0.003	3.21 $\pm$ 0.35	2.07 $\pm$ 0.19	0.02 $\pm$ 0.001	1.12 $\pm$ 0.12	8.35 $\pm$ 0.10	88.97 $\pm$ 18.85
		Arm collector	15.73 $\pm$ 1.02	0.46 $\pm$ 0.002	3.54 $\pm$ 0.29	1.84 $\pm$ 0.12	0.02 $\pm$ 0.001	1.17 $\pm$ 0.12	8.48 $\pm$ 0.03	98.67 $\pm$ 13.35
0.20	60	Porous media	36.43 $\pm$ 3.30	0.77 $\pm$ 0.003	5.14 $\pm$ 1.17	4.18 $\pm$ 0.39	0.04 $\pm$ 0.001	2.94 $\pm$ 0.94	8.51 $\pm$ 0.10	119.46 $\pm$ 17.35
		Domes	54.19 $\pm$ 5.26	0.77 $\pm$ 0.007	2.37 $\pm$ 0.39	6.17 $\pm$ 0.60	0.04 $\pm$ 0.001	0.96 $\pm$ 0.15	8.70 $\pm$ 0.07	17.89 $\pm$ 12.10
		Arm collector	55.45 $\pm$ 8.50	0.77 $\pm$ 0.005	3.72 $\pm$ 0.71	6.51 $\pm$ 1.01	0.04 $\pm$ 0.001	2.01 $\pm$ 0.43	8.56 $\pm$ 0.05	-42.36 $\pm$ 13.93
0.30	30	Porous media	92.12 $\pm$ 21.53	0.45 $\pm$ 0.002	1.76 $\pm$ 1.18	10.76 $\pm$ 2.50	0.01 $\pm$ 0.002	0.40 $\pm$ 0.24	8.50 $\pm$ 0.05	-60.17 $\pm$ 167.60
		Domes	39.82 $\pm$ 4.89	0.45 $\pm$ 0.002	2.60 $\pm$ 0.53	4.81 $\pm$ 0.59	0.02 $\pm$ 0.001	0.90 $\pm$ 0.20	8.22 $\pm$ 0.04	142.28 $\pm$ 20.41
		Arm collector	37.14 $\pm$ 3.95	0.46 $\pm$ 0.002	2.23 $\pm$ 0.46	4.59 $\pm$ 0.49	0.02 $\pm$ 0.001	0.85 $\pm$ 0.21	8.11 $\pm$ 0.13	59.39 $\pm$ 13.60
0.30	60	Porous media	33.10 $\pm$ 2.57	0.68 $\pm$ 0.017	2.97 $\pm$ 0.27	4.08 $\pm$ 0.32	0.04 $\pm$ 0.001	1.40 $\pm$ 0.10	8.01 $\pm$ 0.10	50.58 $\pm$ 8.06
		Domes	24.22 $\pm$ 1.40	0.75 $\pm$ 0.008	4.14 $\pm$ 0.23	3.00 $\pm$ 0.17	0.05 $\pm$ 0.001	2.15 $\pm$ 0.13	7.94 $\pm$ 0.04	24.09 $\pm$ 4.70
		Arm collector	33.66 $\pm$ 1.60	0.76 $\pm$ 0.006	2.76 $\pm$ 0.17	4.38 $\pm$ 0.21	0.04 $\pm$ 0.001	1.27 $\pm$ 0.08	7.67 $\pm$ 0.06	19.72 $\pm$ 7.75

Table 5. Significance level (p-value) of the statistical model and of each factor and interaction for explaining dissolved oxygen and turbidity removal efficiencies and retained mass during the experiment.

	Removal efficiency (%)		Retained mass per cycle (g)
	Dissolved oxygen	Turbidity	
<b>Model</b>	<0.001	<0.001	<0.001
<b>Underdrain design</b>	<0.010	<0.001	<0.001
<b>Media height</b>	<0.010	n.s	<0.001
<b>Filtration velocity</b>	<0.001	<0.001	n.s
<b>Underdrain design x media height</b>	n.s	<0.010	<0.001
<b>Media height x filtration velocity</b>	n.s	<0.001	n.s
<b>Underdrain design x filtration velocity</b>	<0.050	n.s	n.s
<b>Underdrain design x media height x filtration velocity</b>	n.s	<0.001	<0.010
<b>Inlet dissolved oxygen</b>	<0.001	-	-
<b>Inlet turbidity</b>	-	<0.001	<0.001

n.s.: no significant (p>0.050); - : not included in the model

Table 6. Significance level (p-value) of the statistical model and of each factor and interaction for explaining volume and energy parameters variability during the experiment.

	Filtered volume per filtration cycle (m <sup>3</sup> )	Filtered volume/total electrical consumption (m <sup>3</sup> kW h <sup>-1</sup> )
<b>Model</b>	<0.001	<0.001
<b>Underdrain design</b>	<0.001	<0.050
<b>Media height</b>	<0.001	<0.001
<b>Filtration velocity</b>	n.s	<0.010
<b>Underdrain design x media height</b>	<0.001	n.s
<b>Media height x filtration velocity</b>	<0.001	<0.001
<b>Underdrain design x filtration velocity</b>	<0.001	<0.050
<b>Underdrain design x media height x filtration velocity</b>	n.s	n.s
<b>Inlet turbidity</b>	<0.001	n.s

n.s.: no significant (p>0.050)